 CMC, vol.45, no.2, pp.75-105, 2015

Dynamics of the Moving Load Acting on the Hydro-elastic System Consisting of the Elastic Plate, Compressible Viscous Fluid and Rigid Wall

S.D. Akbarov[1,2] **and M.I. Ismailov**[3]

Abstract: The subject of the paper is the study of the dynamics of the moving load acting on the hydro-elastic system consisting of the elastic plate, compressible viscous fluid and rigid wall. Under this study the motion of the plate is described by linear elastodynamics, and the motion of the compressible viscous fluid is described by the linearized Navier-Stokes equations. Numerical results are obtained for the case where the material of the plate is steel, but the fluid material is Glycerin. According to these results, corresponding conclusions related to the influence of the problem parameters, such as fluid viscosity, plate thickness, fluid depth, fluid compressibility and initial stresses on the inter-phase normal stress and normal and tangent velocities of the fluid caused by the load which moves with constant velocity, are made. In particular, it is established that the influence of the fluid viscosity of the aforementioned quantities becomes more considerable under lower velocities of the moving load. Moreover, it is established that there exists a critical velocity of the moving load under which a resonance type event takes place.

Keywords: Moving load, compressible viscous fluid, metal elastic plate, critical velocity, hydro-elastic system.

1 Introduction

Investigations of the dynamics of the hydro-elastic system consisting of the plate and fluid have great significance in the theoretical and application sense in aerospace, nuclear, naval, chemical and biological engineering. The first attempt in

[1] Yildiz Technical University, Faculty of Mechanical Engineering, Department of Mechanical Engineering, Yildiz Campus, 34349, Besiktas, Istanbul-TURKEY. E-mail: akbarov@yildiz.edu.tr
[2] Institute Mathematics and Mechanics of the National Academy of Sciences of Azerbaijan, 37041, Baku, Azerbaijan.
[3] Nachicivan State University, Faculty of Mathematics, Nachicivan, Azerbaijan. E-mail: imeftun@yahoo.com

this field was made in a paper by Lamb (1921) in which vibrations of a circular elastic "baffled" plate in contact with still water were considered. It was assumed that this plate is clamped all around and placed in a matching circular aperture within an infinite rigid plane wall. The investigations were made by the use of the so-called "non-dimensional added virtual mass incremental" (NAVMI) method, according to which, it is assumed that the modes of vibration of the plate in contact with still water are the same as those in a vacuum, and the natural frequency is determined by the use of the Rayleigh quotient. In this case it is supposed that the squares of the natural frequencies of the plate are equal to the ratio between the maximum potential energy of the plate and the sum of the kinetic energies of both the plate and the fluid. Later this method was employed in many related investigations such as in papers by Kwak and Kim (1991), Fu and Price (1987), Zhao and Yu (2012) and many others listed in these papers. Up to now investigations without employing the NAVMI method have also been carried out. For instance, in a paper by Tubaldi and Armabili (2013) the vibration and stability of the rectangular plate immersed in axial liquid flow was studied without employing the NAVMI method, and the Galerkin method was applied to determine the expression of the flow perturbation potential. Then the Rayleigh-Ritz method was used to discretize the system.

Investigations carried out in a paper by Charman and Sorokin (2005) and others listed therein were also made without employing the NAVMI method. Note that in this paper the forced bending vibration of an infinite plate in contact with compressible (acoustic) inviscid fluid, where this fluid occupies a half-space, was considered. This paper gives asymptotic analyses of the sound and vibration in the metal plate and compressible inviscid fluid system.

Another aspect of investigations related to plate-fluid interaction regards wave propagation problems. Investigations carried out in a paper by Sorokin and Chubinskij (2008) and others listed therein provide examples of such problems. It should be noted that before the paper by Sorokin and Chubinskij (2008) the problems of time harmonic linear wave propagation in elastic structure-fluid systems were investigated within the framework of the theory of compressible inviscid fluid. A list and review of these studies are given in the aforementioned paper by Sorokin and Chubinskij (2008). At the same time, the role of fluid viscosity in wave propagation in the plate-fluid system was first investigated in the paper by Sorokin and Chubinskij (2008). However, in this paper and all the papers indicated above, the equations of motion of the plate were written within the scope of the approximate plate theories by the use of various types of hypotheses such as the Kirchhoff hypotheses for plates. Consequently, the use of the approximate plate theories in these investigations decreases the analyzed range of wave modes and their corresponding dispersion curves, significantly. It is evident that in many cases (for instance, in the cases where the wave length is less significant than the thickness of the plate), more accurate results in the qualitative and quantitative sense, can be obtained by employing the exact equations for describing the plate motion. The use of the exact equations of plate motion are taken into consideration in a paper by Bagno et al. (1994) and others, a review of which is given in a survey paper by Bagno and Guz (1997). Note that in these papers, in studying wave propagation in pre-stressed plate + compressible viscous fluid systems, the motion of the plate was written within the scope of the so-called three-dimensional linearized theory of elastic waves in initially stressed bodies. However, the motion of the viscous fluid was written within the scope of the linearized Navier-Stokes equations. Detailed consideration of related results was made in the monograph by Guz (2009).

Until recently, within this framework, there has been no investigation related to the forced vibration of the pre-strained plate + compressible viscous fluid system. The first attempt in this field was made in a work by Akbarov (2013b) in which the frequency response of the system consisting of the pre-stressed metal elastic plate and half-plane occupied with compressible viscous fluid was studied. The subsequent step in this field was made in a paper by Akbarov and Ismailov (2014a) the subject of which was forced vibrations of a system consisting of a pre-stressed highly elastic plate under compressible viscous fluid loading. Moreover, in another paper by Akbarov and Ismailov (2014b) the foregoing investigations were developed for the case where the plate material is viscoelastic. It was assumed that the viscoelasticity is described by fractional exponential operators.

A further considerable aspect of investigations regarding the plate-fluid systems is the dynamic response analysis of plate-fluid systems induced by a moving load. Results of these investigations are applied for construction of floating bridges and for determination of their efficiency. An example of such investigations can be seen in studies carried out in papers by Wu and Shih (1998), Fu et al. (2005), Wang et al. (2009) and others listed therein. However in these investigations the fluid reaction to the plate (i.e. to the floating bridge) is taken into consideration without solution of the equations of the fluid motion. Namely, in these works the so-called hydrostatic force (R) caused by the plate-fluid interaction is determined through the linear spring model, i.e. through the relation $R = -kw$, where w is the vertical displacement of the plate (i.e. the floating bridge) and k is the spring constant. Consequently, in the foregoing investigations, the existence of the fluid is taken into consideration only through this spring constant. It is evident that the approach employed in works by Wu and Shih (1998), Fu et al. (2005) and Wang et al. (2009) is a very approximate one and cannot answer questions about how the fluid viscosity, fluid depth, fluid compressibility, plate thickness and moving velocity of the external force act on the "hydrostatic force" and fluid flow velocities. To find the answers to these questions it is necessary to solve the corresponding coupled fluid-plate interaction problems within the scope of the exact linearized equations described to the plate and fluid motions. In the present paper the first attempt is made for solution to the problems related to the dynamics of the moving load acting on a system consisting of the metal elastic plate, compressible viscous fluid and a rigid wall. The motion of the plate is described by linear elastodynamics, and the motion of the compressible viscous fluid is described by the linearized Navier-Stokes equations.

2 Formulation of the problem

Consider a system consisting of the elastic plate-layer, barotropic compressible Newtonian viscous fluid and rigid wall (Fig. 1). We associate the coordinate system $Ox_1x_2x_3$ with the plate and the position of the points of the constituents we determine in this coordinate system. We consider a motion of the plate-layer in the case where the lineal-located force which moves with the constant velocity V acts on its free face plane. Assume that the plate occupies the region $\{|x_1| < \infty, -h < x_2 < 0\}$, but the fluid occupies the region $\{|x_1| < \infty, -h_d < x_2 < -h\}$.

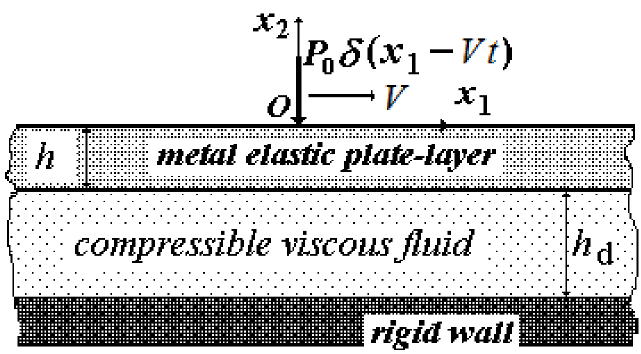

Figure 1: The sketch of the hydro-elastic system under consideration .

Thus, according to the foregoing statement, we can write the following field equations of the linear elastodynamics under the plane-strain state in the Ox_1x_2 plane.

$$\frac{\partial \sigma_{11}}{\partial x_1} + \frac{\partial \sigma_{12}}{\partial x_2} = \rho \frac{\partial^2 u_1}{\partial t^2}, \quad \frac{\partial \sigma_{12}}{\partial x_1} + \frac{\partial \sigma_{22}}{\partial x_2} = \rho \frac{\partial^2 u_2}{\partial t^2}.$$

$$\sigma_{11} = (\lambda + 2\mu)\varepsilon_{11} + \lambda\varepsilon_{22}, \quad \sigma_{22} = \lambda\varepsilon_{11} + (\lambda + 2\mu)\varepsilon_{22}, \quad \sigma_{12} = 2\mu\varepsilon_{12},$$

$$\varepsilon_{11} = \frac{\partial u_1}{\partial x_1}, \quad \varepsilon_{22} = \frac{\partial u_2}{\partial x_2}, \quad \varepsilon_{12} = \frac{1}{2}\left(\frac{\partial u_1}{\partial x_2} + \frac{\partial u_2}{\partial x_1}\right). \tag{1}$$

Note that in Eq. (1) conventional notation is used.

Now, we consider the field equations of motion of the Newtonian compressible viscous fluid: the density, viscosity constants and pressure which are denoted by the upper index (1). Thus, according to Guz (2009), the linearized Navier-Stokes and other field equations for the fluid are:

$$\rho_0^{(1)}\frac{\partial v_i}{\partial t}-\mu^{(1)}\frac{\partial v_i}{\partial x_j\partial x_j}+\frac{\partial p^{(1)}}{\partial x_i}-(\lambda^{(1)}+\mu^{(1)})\frac{\partial^2 v_j}{\partial x_j\partial x_i}=0,\quad \frac{\partial\rho^{(1)}}{\partial t}+\rho_0^{(1)}\frac{\partial v_j}{\partial x_j}=0,$$

$$T_{ij}=\left(-p^{(1)}+\lambda^{(1)}\theta\right)\delta_{ij}+2\mu^{(1)}e_{ij},\quad \theta=\frac{\partial v_1}{\partial x_1}+\frac{\partial v_2}{\partial x_2},$$

$$e_{ij}=\frac{1}{2}\left(\frac{\partial v_i}{\partial x_j}+\frac{\partial v_j}{\partial x_i}\right).\ a_0^2=\frac{\partial p^{(1)}}{\partial\rho^{(1)}}. \tag{2}$$

where $\rho_0^{(1)}$ is the fluid density before perturbation. The other notation used in Eq. (2) is also conventional.

Also, according to Guz (2009), the solution of the system of equations in (2) for 2D plane problems is reduced to finding the two potentials ϕ and ψ which are determined from the following equations:

$$\left[\left(1+\frac{\lambda^{(1)}+2\mu^{(1)}}{a_0^2\rho_0^{(1)}}\frac{\partial}{\partial t}\right)\Delta-\frac{1}{a_0^2}\frac{\partial^2}{\partial t^2}\right]\phi=0,$$

$$\left(\nu^{(1)}\Delta-\frac{\partial}{\partial t}\right)\psi=0,\quad \Delta=\frac{\partial^2}{\partial x_1^2}+\frac{\partial^2}{\partial x_2^2}, \tag{3}$$

where $\nu^{(1)}$ is the kinematic viscosity, i.e. $\nu^{(1)}=\mu^{(1)}\big/\rho_0^{(1)}$.

The velocities v_1 and v_2 and the pressure $p^{(1)}$ are expressed by the potentials ϕ and ψ through the expressions

$$v_1=\frac{\partial\phi}{\partial x_1}+\frac{\partial\psi}{\partial x_2},\quad v_2=\frac{\partial\phi}{\partial x_2}-\frac{\partial\psi}{\partial x_1},\quad p^{(1)}=\rho_0^{(1)}\left(\frac{\lambda^{(1)}+2\mu^{(1)}}{\rho_0^{(1)}}\Delta-\frac{\partial}{\partial t}\right)\phi. \tag{4}$$

Assuming that

$$p^{(1)}=-(T_{11}+T_{22}+T_{33})/3, \tag{5}$$

we obtain:

$$\lambda^{(1)}=-\frac{2}{3}\mu^{(1)}. \tag{6}$$

Moreover, it is assumed that the following boundary, contact and impermeability conditions are satisfied:

$$\sigma_{21}\big|_{x_2=0}=0,\ \sigma_{22}\big|_{x_2=0}=-P_0\delta(x_1-Vt),\quad \left.\frac{\partial u_1}{\partial t}\right|_{x_2=-h}=v_1\big|_{x_2=-h}\quad ,$$

$$\left.\frac{\partial u_2}{\partial t}\right|_{x_2=-h}=v_2\big|_{x_2=-h},\quad \sigma_{21}\big|_{x_2=-h}=T_{21}\big|_{x_2=-h},$$

$$\sigma_{22}\big|_{x_2=-h}=T_{22}\big|_{x_2=-h},\quad v_1\big|_{x_2=-h-h_d}=0,\quad v_2\big|_{x_2=-h-h_d}=0, \tag{7}$$

where $\delta(\cdot)$ is the Dirac delta function.

This completes the formulation of the problem.

3 Method of solution

For the solution of this problem, we use the moving coordinate system $x_1'=x_1-Vt$, $x_2'=x_2$ (below we will omit the upper prime on the new moving coordinates) and, replacing the derivatives $\partial(\bullet)/\partial t$ and $\partial^2(\bullet)/\partial t^2$ with $-V\frac{\partial}{\partial x_1}$ and $V^2\frac{\partial^2}{\partial x_1^2}$, respectively, we obtain the corresponding equations and boundary and contact conditions for the sought values in the moving coordinate system. For the solution to these equations, we employ the exponential Fourier transformation with respect to the x_1 coordinate

$$f_F(s,x_2)=\int_{-\infty}^{+\infty} f(x_1,x_2)e^{-isx_1}dx_1 \tag{8}$$

to these equations. The originals of the sought values can be found through the integrals:

$$\frac{1}{2\pi}\int_{-\infty}^{+\infty}\{u_{1F};u_{2F};\sigma_{11F};\sigma_{12F};\sigma_{22F};v_{1F};v_{2F};T_{11F};T_{12F};T_{22F}\}e^{isx_1}ds \tag{9}$$

Before employing the Fourier transformation (8) we introduce the dimensionless coordinates and dimensionless transformation parameter

$$\bar{x}_1=x_1/h,\quad \bar{x}_2=x_2/h,\quad \bar{s}=sh. \tag{10}$$

Below we will omit the over-bar on the symbols in (10). Moreover, we will also use the notation

$$V'=V/h,\quad \nu^{(1)}=\mu^{(1)}\Big/\rho_0^{(1)}. \tag{11}$$

First, we consider the solution of the equations related to the Fourier transformation of the quantities related to the plate-layer, i.e. the solution of the equations which are obtained from the equations (1) and (9). Thus, substituting the expressions (9) into the equations (1), and doing some mathematical manipulations we obtain the following equations for u_{1F} and u_{2F}.

$$Au_{1F} - B\frac{du_{2F}}{dx_2} + \frac{d^2u_{1F}}{dx_2^2} = 0, \quad Du_{2F} + B\frac{du_{1F}}{dx_2} + G\frac{d^2u_{2F}}{dx_2^2} = 0, \tag{12}$$

where

$$A = X^2 - s^2(\lambda/\mu + 2), \quad B = s(\lambda/\mu + 1), \quad D = s^2(X^2 - 1),$$

$$G = \lambda/\mu + 2, X^2 = V'^2h^2/c_2^2 \quad , \quad c_2 = \sqrt{\mu/\rho} \quad . \tag{13}$$

Introducing the notation

$$A_0 = \frac{AG + B^2 + D}{G}, \quad B_0 = \frac{BD}{G}, \quad k_1 = \sqrt{-\frac{A_0}{2} + \sqrt{\frac{A_0^2}{4} - B_0}} \quad ,$$

$$k_2 = \sqrt{-\frac{A_0}{2} - \sqrt{\frac{A_0^2}{4} - B_0}}, \tag{14}$$

we can write the solution to the equation (12) as follows:

$$u_{2F} = Z_1e^{k_1x_2} + Z_2e^{-k_1x_2} + Z_3e^{k_2x_2} + Z_4e^{-k_2x_2} \quad ,$$

$$u_{1F} = Z_1a_1e^{k_1x_2} + Z_2a_2e^{-k_1x_2} + Z_3a_3e^{k_2x_2} + Z_4a_4e^{-k_2x_2}, \tag{15}$$

where

$$a_1 = \frac{-D - Gk_1^2}{Bk_1^2}, \quad a_2 = -a_1, \quad a_3 = \frac{-D - Gk_2^2}{Bk_2^2}, \quad a_4 = -a_3. \tag{16}$$

Using the equations (1) and (15) we also write expressions for the Fourier transformations σ_{21F} and σ_{22F} of the corresponding stresses which enter the boundary and contact conditions in (7).

$$\begin{aligned}\sigma_{21F} =& Z_1\left(\omega_{2112}k_1a_1 - s\omega_{2121}\right)e^{k_1x_2} + Z_2\left(-\omega_{2112}k_1a_2 - s\omega_{2121}\right)e^{-k_1x_2} \\ &+ Z_3\left(\omega_{2112}k_2a_3 - s\omega_{2121}\right)e^{k_2x_2} + Z_4\left(-\omega_{2112}k_2a_3 - s\omega_{2121}\right)e^{-k_2x_2}, \\ \sigma_{22F} =& Z_1\left(s\omega_{2211}a_1 + k_1\omega_{2222}\right)e^{k_1x_2} + Z_2\left(s\omega_{2211}a_2 - k_1\omega_{2222}\right)e^{-k_1x_2} \\ &+ Z_3\left(s\omega_{2211}a_3 + k_2\omega_{2222}\right)e^{k_2x_2} + Z_2\left(s\omega_{2211}a_4 - k_2\omega_{2222}\right)e^{-k_2x_2}.\end{aligned} \tag{17}$$

This completes consideration of the determination of the Fourier transformation of the values related to the plate-layer. Now we consider determination of the Fourier transformations of the quantities related to the fluid flow. First, we consider the determination of ϕ_F and ψ_F from the Fourier transformation of the equations in (3). Taking the relation

$$\phi_F = -sV'h^2\tilde{\phi}_F, \quad \psi_F = -sV'h^2\tilde{\psi}_F \tag{18}$$

into account, it can be written that

$$\frac{d^2\tilde{\phi}_F}{dx_2^2} + s^2\left(\frac{\Omega_1^2}{1 - i4s\Omega_1^2/(3N_w^2)} - 1\right)\tilde{\phi}_F = 0, \quad \frac{d^2\tilde{\psi}_F}{dx_2^2} - \left(s^2 - isN_w^2\right)\tilde{\psi}_F = 0, \tag{19}$$

where

$$\Omega_1 = \frac{V'h}{a_0}, \quad N_w^2 = \frac{V'h^2}{\nu^{(1)}}. \tag{20}$$

The dimensionless number N_w in (20) can be taken as a Womersley number and characterizes the influence of the fluid viscosity on the mechanical behavior of the system under consideration. For pure hydrodynamic problems, when the Womersley number is large (around 10 or greater), the flow is dominated by oscillatory inertial forces. When the Womersley number is low, viscous forces tend to dominate the flow. However, for hydro-elastodynamic problems the "large" and "low" limits for the Womersley number can change significantly.

The dimensionless frequency Ω_1 in (20) can be taken as the parameter through which the influence of the compressibility of the fluid on the mechanical behavior of the system under consideration can be characterized.

Thus, taking the relation (6) into consideration, the solutions to the equations in (19) are found as follows:

$$\tilde{\phi}_F = Z_5 e^{\delta_1 x_2} + Z_7 e^{-\delta_1 x_2}, \quad \tilde{\psi}_F = Z_6 e^{\gamma_1 x_2} + Z_8 e^{-\gamma_1 x_2}, \tag{21}$$

where

$$\delta_1 = s^2\sqrt{1 - \frac{\Omega_1^2}{1 - i4s\Omega_1^2/(3N_w^2)}} \quad , \quad \gamma_1 = \sqrt{s^2 - isN_w^2}. \tag{22}$$

Using (21) and (18) we obtain the following expressions for the velocities, pressure and stresses of the fluid from the Fourier transformations of the Eqs. (2) and (3).

$$v_{1F} = -sV'h\left[-Z_5 s e^{\delta_1 x_2} - Z_7 s e^{-\delta_1 x_2} + Z_6 e^{\gamma_1 x_2} + Z_8 e^{-\gamma_1 x_2}\right],$$

$$v_{2F} = -sV'h\left[Z_5\delta_1 e^{\delta_1 x_2} - Z_7\delta_1 e^{-\delta_1 x_2} - Z_6 s e^{\gamma_1 x_2} - Z_8 s e^{-\gamma_1 x_2}\right],$$

$$T_{22F} = \mu^{(1)}(-sV')\left[Z_5\left(\frac{4}{3}\delta_1^2 + \frac{2}{3}s^2 - R_0\right)e^{\delta_1 x_2} + Z_7\left(\frac{4}{3}\delta_1^2 + \frac{2}{3}s^2 - R_0\right)e^{-\delta_1 x_2}\right.$$
$$\left. + Z_6\left(-s\gamma_1 - \frac{2}{3}s\gamma_1\right)e^{\gamma_1 x_2} + Z_8\left(s\gamma_1 + \frac{2}{3}s\gamma_1\right)e^{-\gamma_1 x_2}\right],$$

$$T_{21F} = -\mu^{(1)}(-sV')\left[2s\delta_1 Z_5 e^{\delta_1 x_2} - 2s\delta_1 Z_7 e^{-\delta_1 x_2}\right.$$
$$\left. + (s^2+\gamma_1^2)Z_6 e^{\gamma_1 x_2} + (s^2+\gamma_1^2)Z_8 e^{-\gamma_1 x_2}\right]$$

$$p_F^{(1)} = \mu^{(1)}(-sV')R_0\left(Z_5 e^{\delta_1 x_2} + Z_7 e^{-\delta_1 x_2}\right), \tag{23}$$

where

$$R_0 = -\frac{4}{3}\frac{s^2\Omega_1^2}{1 - i4s\Omega_1^2/(3N_w^2)} + isN_w^2. \tag{24}$$

Substituting expressions (15), (17) and (23) into the boundary and contact conditions in (7) we obtain a system of equations with respect to the unknowns Z_1, Z_2,...,Z_8 through which the sought values are determined. These equations can be expressed as follows:

$$\left(\sigma_{21F}/\mu\right)\big|_{x_2=0} = Z_1\alpha_{11} + Z_2\alpha_{12} + Z_3\alpha_{13} + Z_4\alpha_{14} = 0,$$

$$\left(\sigma_{22F}/\mu\right)\big|_{x_2=0} = Z_1\alpha_{21} + Z_2\alpha_{22} + Z_3\alpha_{23} + Z_4\alpha_{24} = -P_0/\mu,$$

$$\left.\frac{\partial u_{1F}}{\partial t}\right|_{x_2=-h} - v_{1F}\big|_{x_2=-h} = -isV'(Z_1\alpha_{31} + Z_2\alpha_{32} + Z_3\alpha_{33} + Z_4\alpha_{34}) -$$
$$+ sV'h(Z_5\alpha_{35} + Z_6\alpha_{36} + Z_7\alpha_{37} + Z_8\alpha_{38}) = 0,$$

$$\left.\frac{\partial u_{2F}}{\partial t}\right|_{x_2=-h} - v_{2F}\big|_{x_2=-h} = -isV'(Z_1\alpha_{41} + Z_2\alpha_{42} + Z_3\alpha_{43} + Z_4\alpha_{44}) -$$
$$+ sV'h(Z_5\alpha_{45} + Z_6\alpha_{46} + Z_7\alpha_{47} + Z_8\alpha_{48}) = 0,$$

$$\left(\sigma_{21}/\mu\right)\big|_{x_2=-h} - \left(T_{21}/\mu\right)\big|_{x_2=-h} = Z_1\alpha_{51} + Z_2\alpha_{52} + Z_3\alpha_{53} + Z_4\alpha_{54} +$$
$$Ms(Z_5\alpha_{55} + Z_6\alpha_{56} + Z_7\alpha_{57} + Z_8\alpha_{58}) = 0,$$

$$\left(\sigma_{22}/\mu\right)\big|_{x_2=-h} - \left(T_{22}/\mu\right)\big|_{x_2=-h} = Z_1\alpha_{61} + Z_2\alpha_{62} + Z_3\alpha_{63} + Z_4\alpha_{64} +$$
$$Ms(Z_5\alpha_{65} + Z_6\alpha_{66} + Z_7\alpha_{67} + Z_8\alpha_{68}) = 0,$$

$$v_{1F}\big|_{x_2=-h-h_d} = -sV'h(Z_5\alpha_{75} + Z_6\alpha_{76} + Z_7\alpha_{77} + Z_8\alpha_{78}) = 0,$$

$$v_{2F}|_{x_2=-h-h_d} = -sV'h(Z_5\alpha_{85} + Z_6\alpha_{86} + Z_7\alpha_{87} + Z_8\alpha_{88}) = 0 \tag{25}$$

where

$$M = \frac{\mu^{(1)}V'}{\mu h}. \tag{26}$$

The expressions of the coefficients $\alpha_{nm}(n;m = 1,2,...,8)$ can be easily determined from the Eqs. (15), (17) and (23), and therefore they are not given here. Thus, the unknowns $Z_1, Z_2, ..., Z_8$ in the Eq. (25) can be determined via the formula

$$Z_k = \frac{\det\|\beta_{nm}^k\|}{\det\|\alpha_{nm}\|}. \tag{27}$$

Note that the matrix (β_{nm}^k) is obtained from the matrix (α_{nm}) by replacing the $k-th$ column of the latter with the column $(0,-P_0/\mu,0,0,0,0,0,0)^T$.

Now we consider calculation of the integrals in Eq. (9). For this purpose, firstly we consider the following reasoning. If we take the Fourier transformation parameter s as the wavenumber, then the equation

$$\det\|\alpha_{nm}\| = 0, \quad n;m = 1,2,...,8, \tag{28}$$

coincides with the dispersion equation of the waves with the velocity V propagated in the direction of the Ox_1 axis in the system under consideration. It should be noted that, according to well-known physico-mechanical considerations, the equation (28) must have complex roots only for the system under consideration. This character of the roots is caused by the viscosity of the fluid. However, as usual, the viscosity of the Newtonian fluids is insignificant in the qualitative sense and therefore in some cases within the scope of the necessity of the accuracy of the PC calculation, the equation (28) may have "real roots". Consequently, these roots become singular points of the integrated expressions in the integrals (9) and for such cases the algorithm for calculation was discussed in papers by Akbarov (2013a), Akbarov et al. (2013), Akbarov and Ilhan (2013), and other works listed therein. Moreover, the algorithm was also detailed in a monograph by Akbarov (2015), according to which, in these cases the wavenumber integrals (9) may be evaluated along the Sommerfeld contour. However, in the present investigations under calculation of the integrals in (9) the aforementioned "real roots" cases did not arise and according to expression (9), the sought values are determined through the following relation:

$$\{u_1;u_2;\sigma_{11};\sigma_{12};\sigma_{22};v_1;v_2;T_{11};T_{12};T_{22}\} = \frac{1}{2\pi}Re\left[\int_{-\infty}^{+\infty}\{u_{1F};u_{2F};\sigma_{11F};\right.$$
$$\left.\sigma_{12F};\sigma_{22F};v_{1F};v_{2F};T_{11F};T_{12F};T_{22F}\}e^{isx_1}ds\right]. \tag{29}$$

The algorithms employed for calculation of the integrals in the form (29) will be discussed in the next section. Note that after some obvious changes the foregoing solution method can also be applied for the case where the fluid is inviscid.

4 Numerical results and discussions

It follows from the foregoing discussions that the problem under consideration is characterized through the dimensionless parameters Ω_1 and N_w, which are determined by the expressions in (20) and M which is determined by the expression (26) and λ/μ, λ and μ are the mechanical constants which enter the expression of the elastic relations in Eq. (1). Note that the case where $\Omega_1 = 0$ corresponds to the case where the fluid is incompressible, but the case where $1/N_w = 0$ corresponds to the case where the fluid is inviscid.

In the numerical investigation, according to Guz (2004, 2009), and Guz and Makhort (2000), we assume that the material of the plate-layer is Steel with mechanical constants $\mu = 79 \times 10^9 Pa$, $\lambda = 94.4 \times 10^9 Pa$, and density $\rho = 1160 kg/m^3$, but the material of the fluid is Glycerin with viscosity coefficient $\mu^{(1)} = 1,393 kg/(m \cdot s)$, density $\rho = 1260 kg/m^3$and sound speed $a_0 = 1927 m/s$. We also introduce the notation $c_2 = \sqrt{\mu/\rho}$ which is the shear wave propagation velocity in the layer material in the case where the initial strains are absent.

Thus, after selection of these materials, the foregoing dimensionless parameters can be determined through the three quantities: h (the thickness of the plate-layer), h_d (the thickness of the fluid strip) and V (the velocity of the external moving load). One of the main parameters for the problem under consideration is h_d/h. Namely, through this parameter we will estimate the influence of the fluid depth on the dynamic behavior of the hydro-elastic system. Numerical results which will be discussed below relate to the normal stress acting on the interface plane between the fluid and plate-layer and to the velocities of the fluid (or of the plate-layer) on the interface plane in the directions of the Ox_1 and Ox_2 axes (Fig. 1). Discussions related to the results illustrating the influence of the fluid viscosity and the fluid compressibility on the studied quantities will be made separately. However we begin discussions of the numerical results with consideration of the calculation algorithm and its convergence.

4.1 Convergence of the numerical algorithm

Under obtaining numerical results, which will be discussed below, the integral $\int_{-\infty}^{+\infty} (\bullet) ds$ in the expression (29) is replaced with $\int_{-S_1^*}^{+S_1^*} (\bullet) ds$, i.e. it is assumed that $\int_{-\infty}^{+\infty} (\bullet) ds \approx \int_{-S_1^*}^{+S_1^*} (\bullet) ds$. The values of S_1^* are determined from the convergence criterion of the calculated integrals in (29). The results obtained for various problem parameters show that the very disadvantaged case, in the convergence sense, appears for the thinner plate under low velocity of the moving load and under small values of the ratio h_d/h. Therefore, for illustration of this convergence we consider the case where $h = 0.01m$, $4hz \le V' \le 2000hz$, $h_d/h = 2$ and $x_1/h = -20.0$. Under calculation of the related integrals, the interval $[-S_1^*, +S_1^*]$ is divided into a certain number of shorter intervals. Let us denote this number through $2N$. Consequently, the length of these shorter intervals is S_1^*/N and in each of these shorter intervals the integration is made by the use of the Gauss integration algorithm with ten sample points. Consequently, convergence of the numerical integration can be estimated with respect to the values of S_1^* and N.

Thus, we consider examples of the convergence of the numerical results with respect to the aforementioned number N in the case where $S_1^* = 5$. Analyze the graphs given in Fig.2 which illustrate the response of the dimensionless stress $T_{22}h/P_0$ (Fig. 2a) and dimensionless velocities $v_2\mu h/(P_0c_2)$ (Fig. 2b) and $v_1\mu h/(P_0c_2)$ (Fig. 2c) to the moving load velocity $V/h\ (= V')$ under $x_1/h = -20.0$. Note that under construction of these graphs (as well as all graphs which will be discussed below) the values of the velocities and stress are calculated on the interface plane (i.e. at $x_2 = -h$) between the fluid and the plate.

It follows from Fig. 2 that the values of the velocities and stress approach a certain asymptote with the number N. In other words, the numerical results obtained for the studied quantities approach a certain limit with the number N and that after a certain value of N (denote it by N^*) the numerical results obtained for the various $N > N^*$ coincide with each other with accuracy $10^{-5} - 10^{-6}$. It should be noted that the value of N^* depends not only on the velocity of the moving load, but also on the other problem parameters and mainly on h and h_d/h. For instance, for the case under consideration it can be taken that $N^* = 2000$.

Consider also the graphs which illustrate the convergence of the numerical results with respect to the integrating interval, i.e. with respect to the values of S_1^*. These graphs are given in Fig. 3a for the dimensionless stress $T_{22}h/P_0$, and in Figs. 3b and 3c for the dimensionless velocities $v_2\mu h/(P_0c_2)$ and $v_1\mu h/(P_0c_2)$, respectively. Under construction of these graphs it is assumed that $N = 2000$, $h_d/h = 2$ and $x_1/h = -20.0$.

It follows from these graphs that the numerical results approach a certain asymptote with S_1^*, and with the velocity V', the convergence of the numerical results with respect to S_1^* requires an increase in the values of S_1^*.

In obtaining the numerical results, which will be discussed below, all the foregoing particularities relating to the convergence of the numerical results are taken into

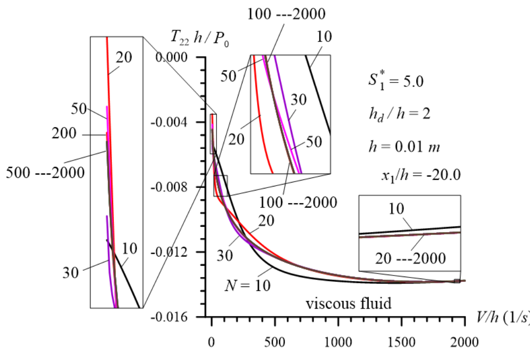

(a)

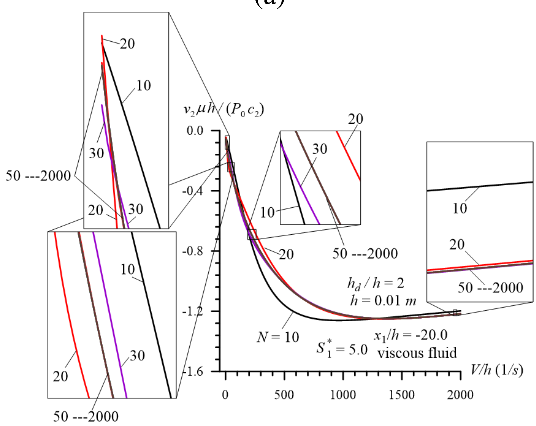

(b)

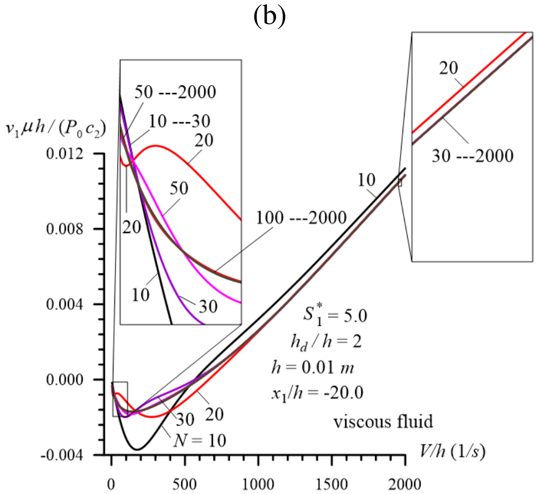

(c)

Figure 2: The illustration of the convergence of the numerical results related to $T_{22}h/P_0$ (a), $v_2\mu h/(P_0c_2)$(b) and $v_1\mu h/(P_0c_2)$(c) with respect to number N, which are obtained in the case where $h = 0.01\,m$, $h_d/h = 2$, $S_1^* = 5$ and $x_1/h = -20.0$.

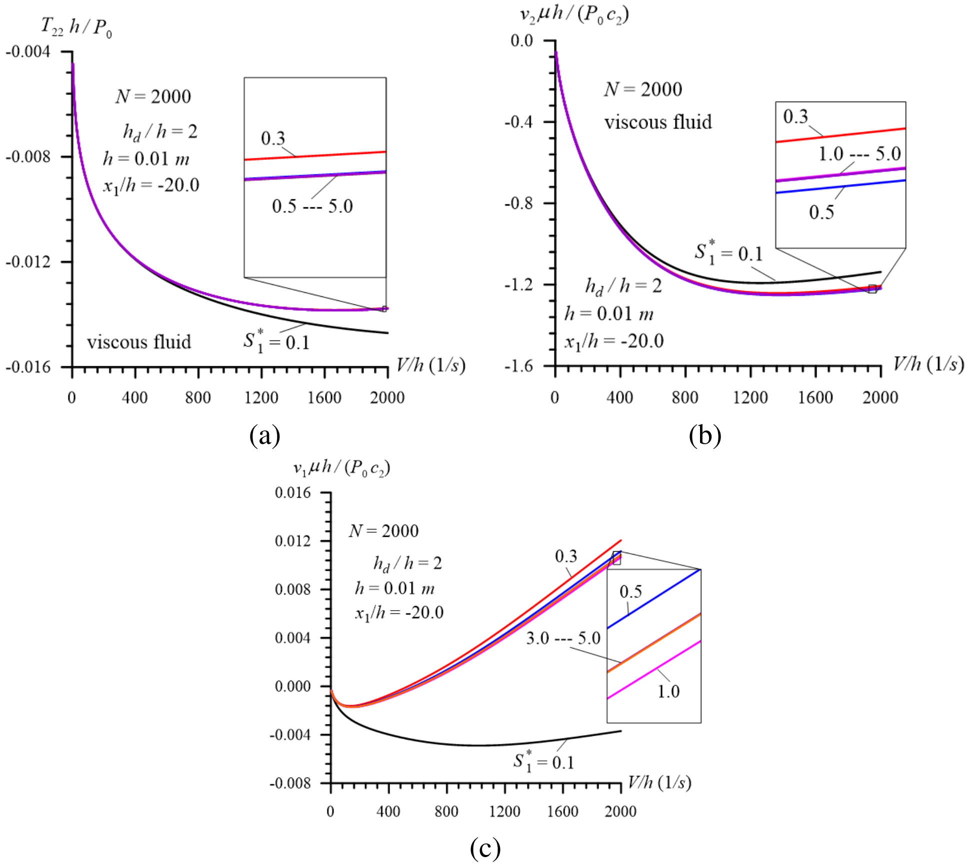

Figure 3: The illustration of the convergence of the numerical results related to $T_{22}h/P_0$ (a), $v_2\mu h/(P_0c_2)$(b) and $v_1\mu h/(P_0c_2)$(c) with respect to number S_1^*which are obtained in the case where $h = 0.01\,m$, $h_d/h = 2$, $N = 2000$ and $x_1/h = -20.0$

consideration and it is established that the case where $S_1^* = 5$ and $N = 2000$ is quite sufficient for obtaining verified results. Therefore in obtaining the numerical results presented in the present paper we assume that $S_1^* = 5$ and $N = 2000$. At the same time, it should be noted that the foregoing convergence results can also be taken as validation of the algorithm and programs used. Unfortunately, we have not found any related results of other authors in order to compare with the present ones. Therefore validation of the present results can be proven with the convergence of the numerical results and with the consistency of the results with mechanical considerations.

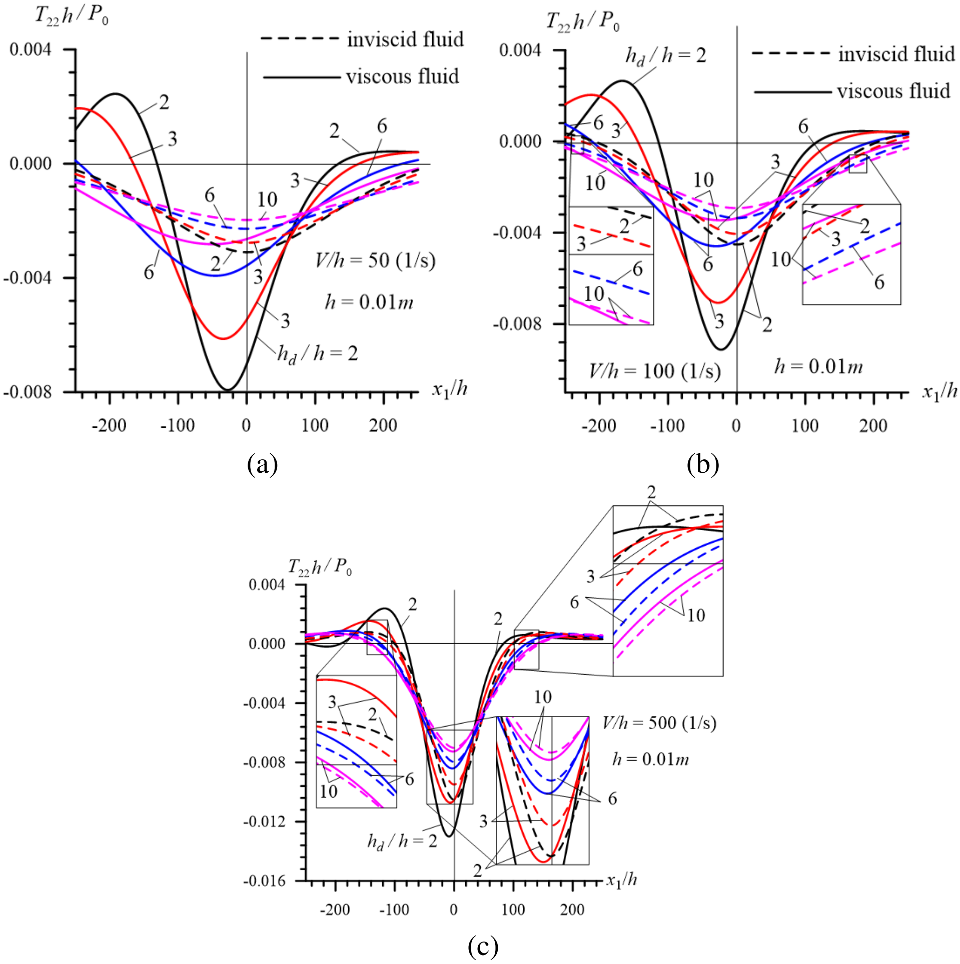

Figure 4: The distribution of the stress $T_{22}h/P_0$ with respect to the dimensionless moving coordinate x_1/h under $h = 0.01\,m$, $h_d/h = 2$ in the cases where $V/h = 50\,(1/s)$ (a), 100 $(1/s)$ (b) and 500 $(1/s)$ (c)

4.2 The influence of the fluid viscosity on the distribution of the interface stress and velocities

First we investigate the distribution of the studied quantities $T_{22}h/P_0$, $v_2\mu h/(P_0c_2)$ and $v_1\mu h/(P_0c_2)$ on the interface plane with respect to the dimensionless coordinate $x_1\big/h$. We recall that here the coordinate x_1 is determined with respect to the moving coordinate system and, according to the coordinate transformation $x_1' = x_1 - Vt$,

$x_2' = x_2$ which was introduced in the beginning of the previous section (the upper prime over the moving coordinates was omitted), the change in the values of x_1/h (i.e. of x_1'/h) can also be considered as a change in the values of the dimensionless time Vt/h. Consequently, the distribution of the foregoing quantities with respect to the moving dimensionless coordinate x_1/h can also be considered as the change at some fixed point in the frame of the fixed coordinate system with respect to the dimensionless time Vt/h.

According to the foregoing reason and to the fact that in the hydro-elastic system which contains a viscous fluid, there exists a phase shifting between the external forces and responses as well as between the velocities and stresses. Thus, we can make the following prediction: if the distribution of some quantities obtained for the hydro-elastic system containing the inviscid fluid with respect to the dimensionless moving coordinate x_1/h is symmetric (or asymmetric) with respect to the point $x_1/h = 0$, then this symmetry (or asymmetry) must be violated for the same distribution obtained for the same hydro-elastic system containing the corresponding viscous fluid. It is evident that this violation will become more considerable with decreasing values of the dimensionless parameter N_w (20) (Womersley number). Consequently, if we increase the values of the plate thickness h for a fixed velocity of the moving load, or if we increase the velocity of the moving load for a fixed plate thickness then the aforementioned symmetry or asymmetry violation must decrease.

Thus, taking the foregoing mechanical considerations into account, consider the numerical results related to the distribution of the studied quantities with respect to the dimensionless moving coordinate x_1/h. Graphs of these distributions are given in Figs. 4 (for $T_{22}h/P_0$), 5 (for $v_2\mu h/(P_0c_2)$), 6 (for $v_1\mu h/(P_0c_2)$ in the viscous fluid case) and 7 (also for $v_1\mu h/(P_0c_2)$ in the inviscid fluid case). Note that these graphs are constructed in the case where $h = 0.01m$ for various values of the ratio h_d/h and for various values of the velocity V/h. The graphs grouped by the letters a, b and c relate to the cases where V/h =50 (1/s), 100 (1/s) and 500 (1/s), respectively. In Figs. 4 and 5 the results related to the viscous and corresponding inviscid fluid cases are given simultaneously. Here and below under "inviscid fluid case" ("viscous fluid case") we will understand the case where the selected fluid (i.e. Glycerin) is modeled as inviscid (viscous). However, the results obtained for $v_1\mu h/(P_0c_2)$ in the viscous fluid case are incompatible with those obtained in the inviscid fluid case. Therefore the results obtained for $v_1\mu h/(P_0c_2)$ in the viscous and inviscid fluid cases are given separately in Figs. 6 and 7, respectively. This incompatibility can be explained with the disappearance of the contact condition $\partial u_1/\partial t\big|_{x_2=-h} = v_1\big|_{x_2=-h}$ and the impermeability condition $v_1\big|_{x_2=-h-h_d} = 0$ in (7) for the inviscid fluid case.

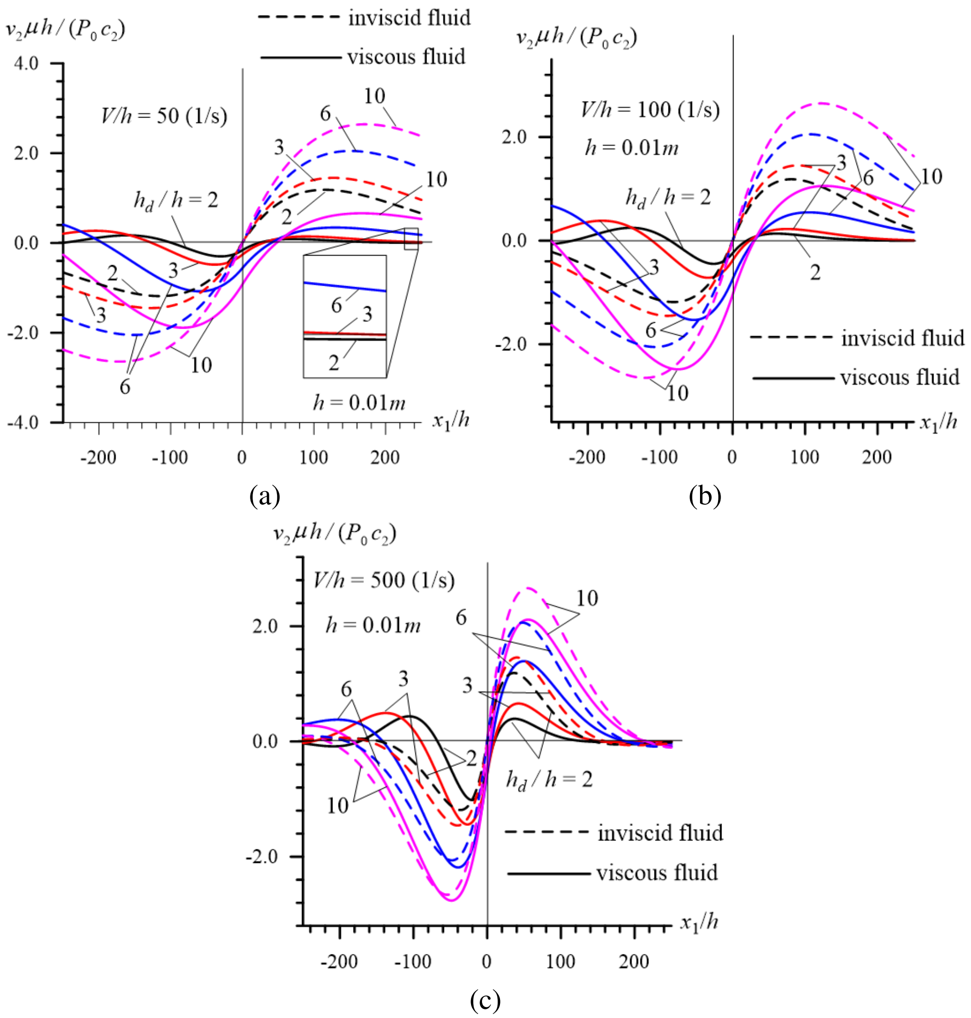

Figure 5: The distribution of the velocity $v_2\mu h/(P_0c_2)$ with respect to the dimensionless moving coordinate x_1/h under $h = 0.01\,m$, $h_d/h = 2$ in the cases where $V/h = 50\,(1/s)$ (a), 100 $(1/s)$ (b) and 500 $(1/s)$ (c)

It follows from the analysis of the graphs that in the inviscid fluid case the distribution of the stress $T_{22}h/P_0$ and velocity $v_1\mu h/(P_0c_2)$ with respect to x_1/h is symmetric, but the same distribution of the velocity $v_2\mu h/(P_0c_2)$ is asymmetric with respect to the point $x_1/h = 0$. However, this symmetry and asymmetry is violated in the viscous fluid case. The absolute maximum values of the stress $T_{22}h/P_0$

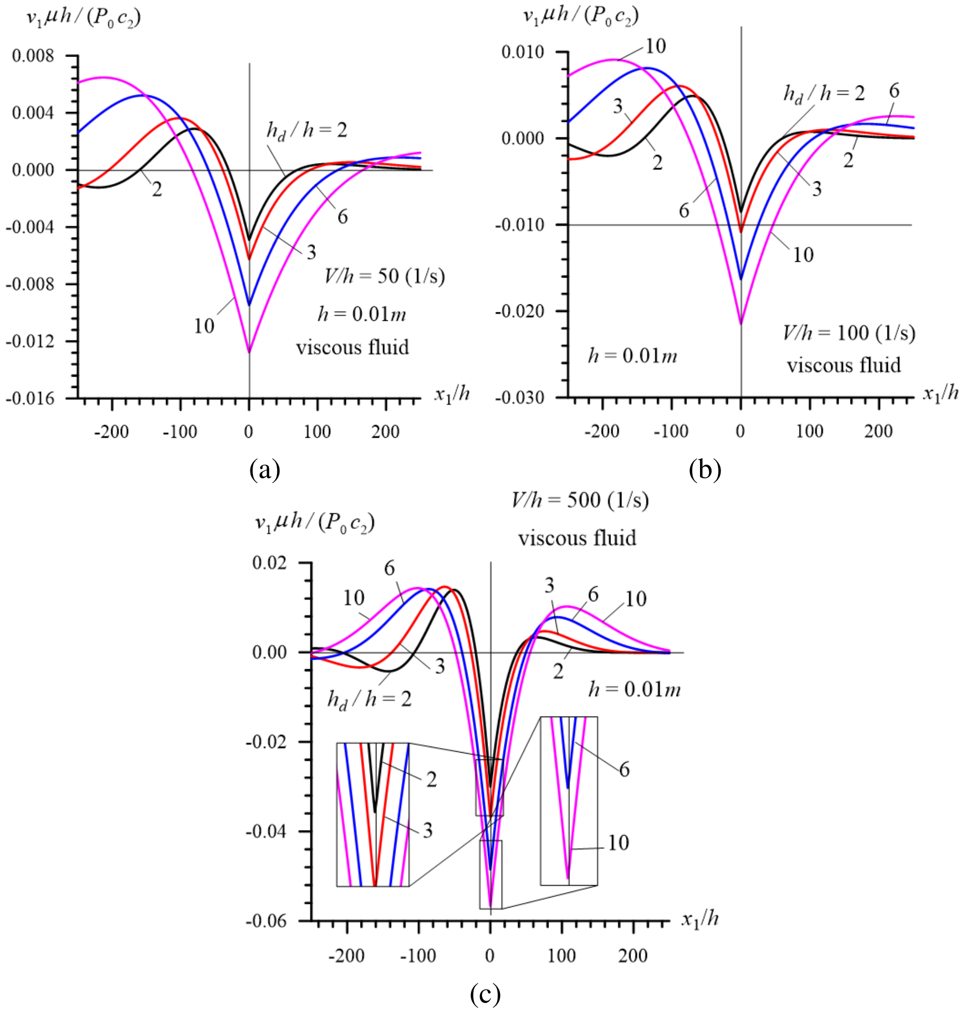

Figure 6: The distribution of the velocity $v_1\mu h/(P_0c_2)$ with respect to the dimensionless moving coordinate x_1/h for the viscous fluid case under $h=0.01\,m$, $h_d/h=2$ in the cases where $V/h=50\,(1/s)$ (a), 100 $(1/s)$ (b) and 500 $(1/s)$ (c)

and velocity $v_2\mu h/(P_0c_2)$ in the viscous fluid case appear behind the moving load, i.e. at $x_1/h<0$, but absolute maximum values of the velocity $v_1\mu h/(P_0c_2)$ appear at point $x_1/h=0$. The values of the stress $T_{22}h/P_0$ decrease but the values of the velocity $v_2\mu h/(P_0c_2)$ increase with h_d/h. At the same time, the values of the velocity $v_1\mu h/(P_0c_2)$ in the viscous fluid case also increase, but in the inviscid fluid

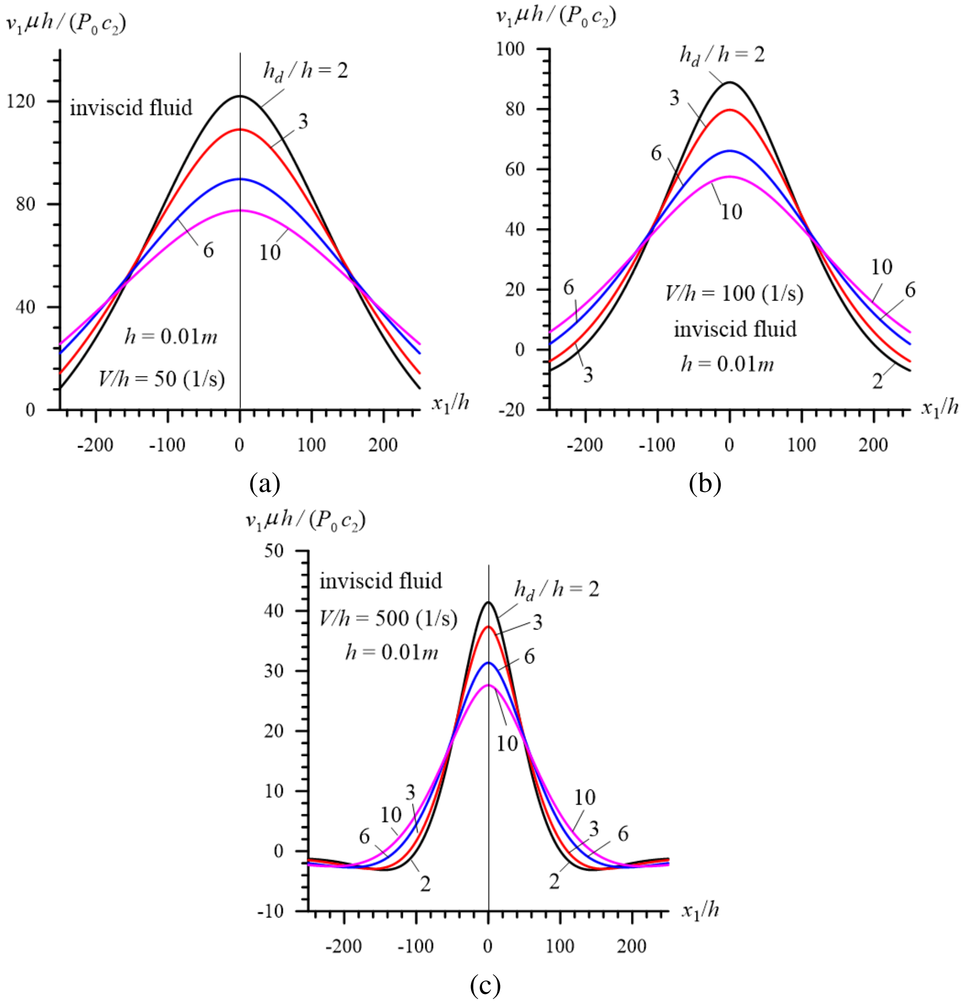

Figure 7: The distribution of the velocity $v_1\mu h/(P_0c_2)$ with respect to the dimensionless moving coordinate x_1/h for the inviscid fluid case under $h = 0.01\,m$, $h_d/h = 2$ in the cases where $V/h = 50\,(1/s)$ (a), 100 $(1/s)$ (b) and 500 $(1/s)$ (c)

case, they decrease with the ratio h_d/h. Moreover, the results show that the fluid viscosity causes the absolute values of the stress $T_{22}h/P_0$ to increase, but the absolute values of the velocity $v_2\mu h/(P_0c_2)$ to decrease. However, the values of the velocity $v_1\mu h/(P_0c_2)$ obtained in the viscous fluid case are not comparable with the corresponding ones obtained in the inviscid fluid case. Consequently, according to

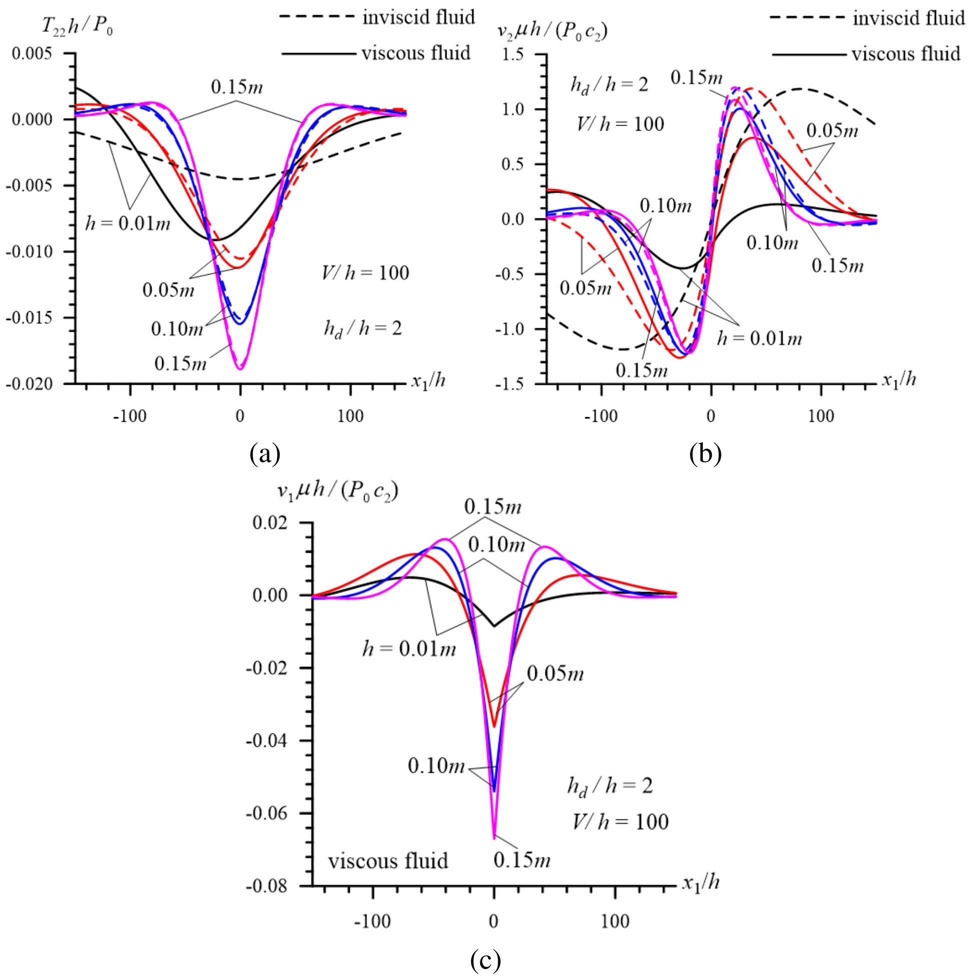

Figure 8: The influence of the plate thickness h on the distribution of the stress $T_{22}h/P_0$(a) and velocities $v_2\mu h/(P_0c_2)$ (b) and $v_1\mu h/(P_0c_2)$ (c) with respect to the dimensionless moving coordinate x_1/h in the case where $V/h = 100\,(1/s)$and $h_d/h = 2$

the results given in Figs. 6 and 7, we can conclude that the distribution of the velocity $v_1\mu h/(P_0c_2)$ cannot be described within the scope of the inviscid fluid model either in the quantitative sense or in the qualitative sense.

The analysis of the results given in the figures indicated by the letters a, b and c allow us to conclude that the difference between the results obtained for the stress

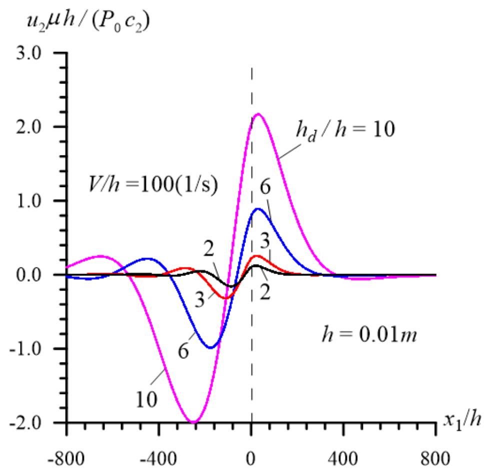

Figure 9: The distribution of the displacement $u_2\mu h/(P_0c_2)$ with respect to the dimensionless moving coordinate x_1/h under $h = 0.01\,m$ for various values of h_d/h in the cases where $V/h = 100\,(1/s)$

$T_{22}h/P_0$ and for the velocity $v_2\mu h/(P_0c_2)$ in the viscous and inviscid fluid cases decreases with the velocity V/h of the moving load. At the same time, this analysis shows that the attenuation of the investigated quantities with $|x_1/h|$ takes place more rapidly and the width of the action area of the moving load decreases with increasing V/h.

Now we investigate how the increase of the plate thickness acts on the character of the foregoing distribution under fixed V/h. For this purpose we consider the graphs given in Fig. 8 which show the distribution of $T_{22}h/P_0$(Fig.8a), $v_2\mu h/(P_0c_2)$(Fig.8b) and $v_1\mu h/(P_0c_2)$(Fig. 8c) with respect to x_1/h for various values of the plate thickness h in the case where $V/h = 100\,(1/s)$ and $h_d/h = 2$. It follows from these graphs that the influence of the fluid viscosity on the distributions under considerations weakens with the plate thickness h. Consequently, all the predictions based on the mechanical considerations made in the first two paragraphs of the present subsection are proven with the concrete numerical results given in Figs. 4 - 8.

We again note that the foregoing results can also be estimated as the change of the studied quantities with respect to time at a certain fixed point of the interface plane. For instance, we consider a point which is at a distance L from the origin of the fixed coordinate system. According to the relation $x_1 = L - Vt = 0$, we determine the time $t* = L/V$ at which the moving load achieves this point. Consequently, the

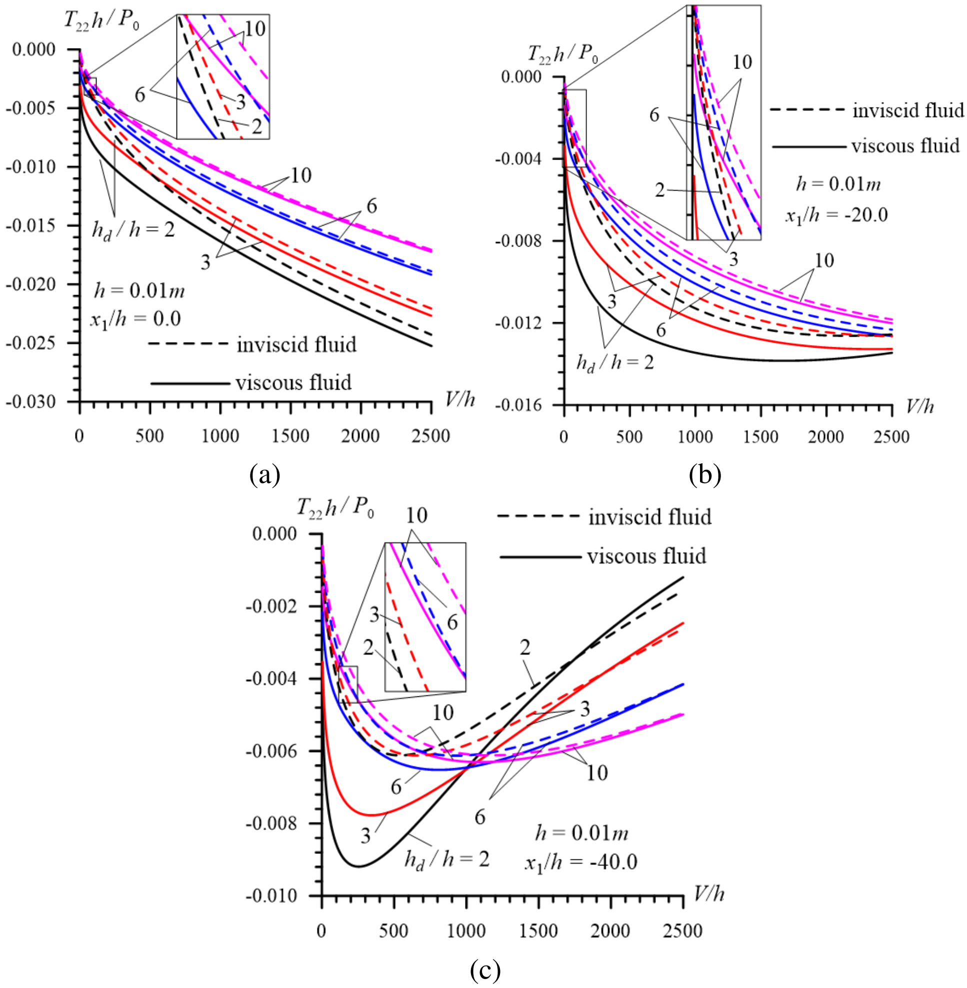

Figure 10: The graphs of the dependence between the stress $T_{22}h/P_0$ and velocity of the moving load V/h calculated at $x_1/h = 0.0$ (a), -20.0 (b) and -40.0 (c) in the case where $h = 0.01\,m$ for various values of h_d/h

left (right) branch of the graphs given in Figs. 4 – 8 which illustrate the change of the studied quantities with respect to x_1/h under $x_1/h \leq 0$ (under $x_1/h \geq 0$) can also be taken as the change with respect to time t under $t \geq t*$ (under $t \leq t*$) at the point which is at a distance L from the origin of the fixed coordinate system.

In the aforementioned sense it is also interesting to consider the distribution of the displacement of the interface plane with respect to x_1/h, namely because through

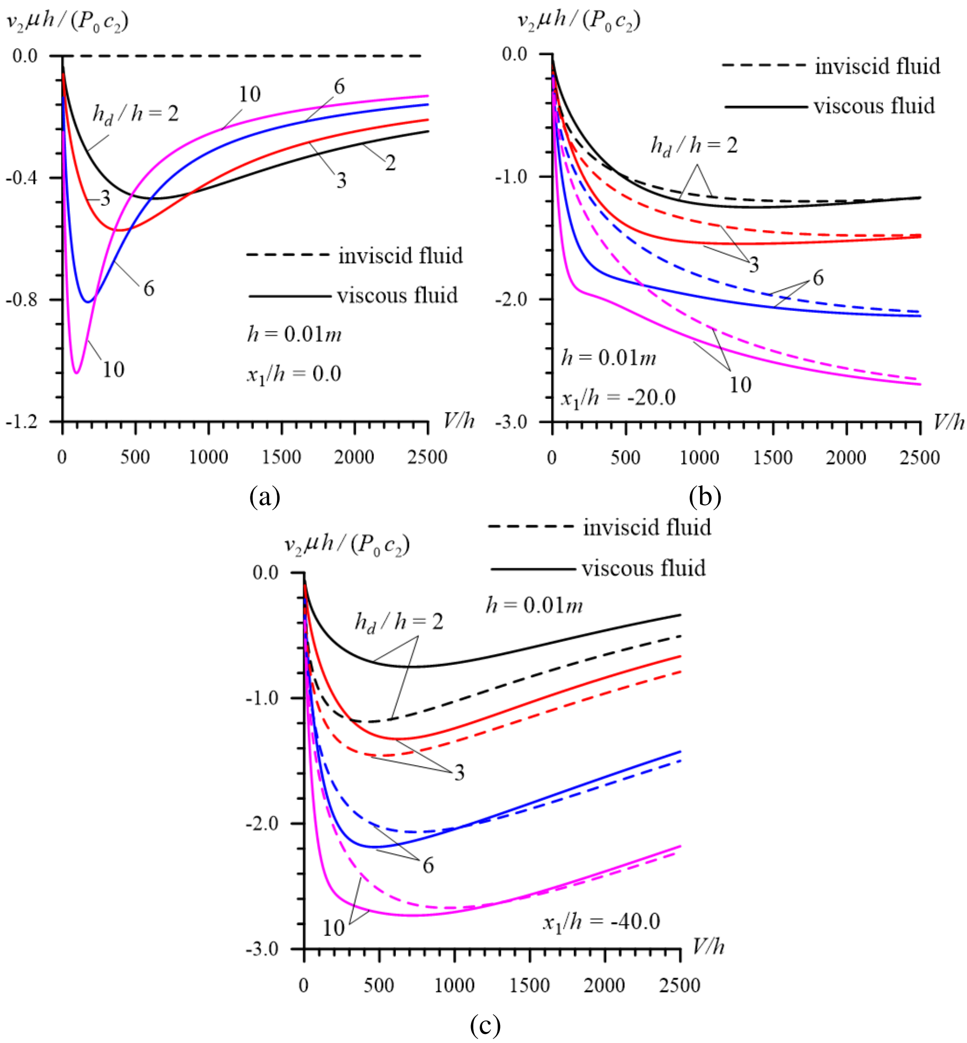

Figure 11: The graphs of the dependence between the velocity $v_2\mu h/(P_0c_2)$ and velocity of the moving load V/h calculated at $x_1/h = 0.0$ (a), -20.0 (b) and -40.0 (c) in the case where $h = 0.01\,m$ for various values of h_d/h

these distributions we can make some estimations on the attenuation of the action of the moving vehicles with time. As an example of such a distribution are the graphs given in Fig. 9 which illustrate the dependence between $u_2\mu h/(P_0c_2)$ and x_1/h constructed for various h_d/h in the case where $V/h = 100\,(1/s)$ under $h = 0.01m$.

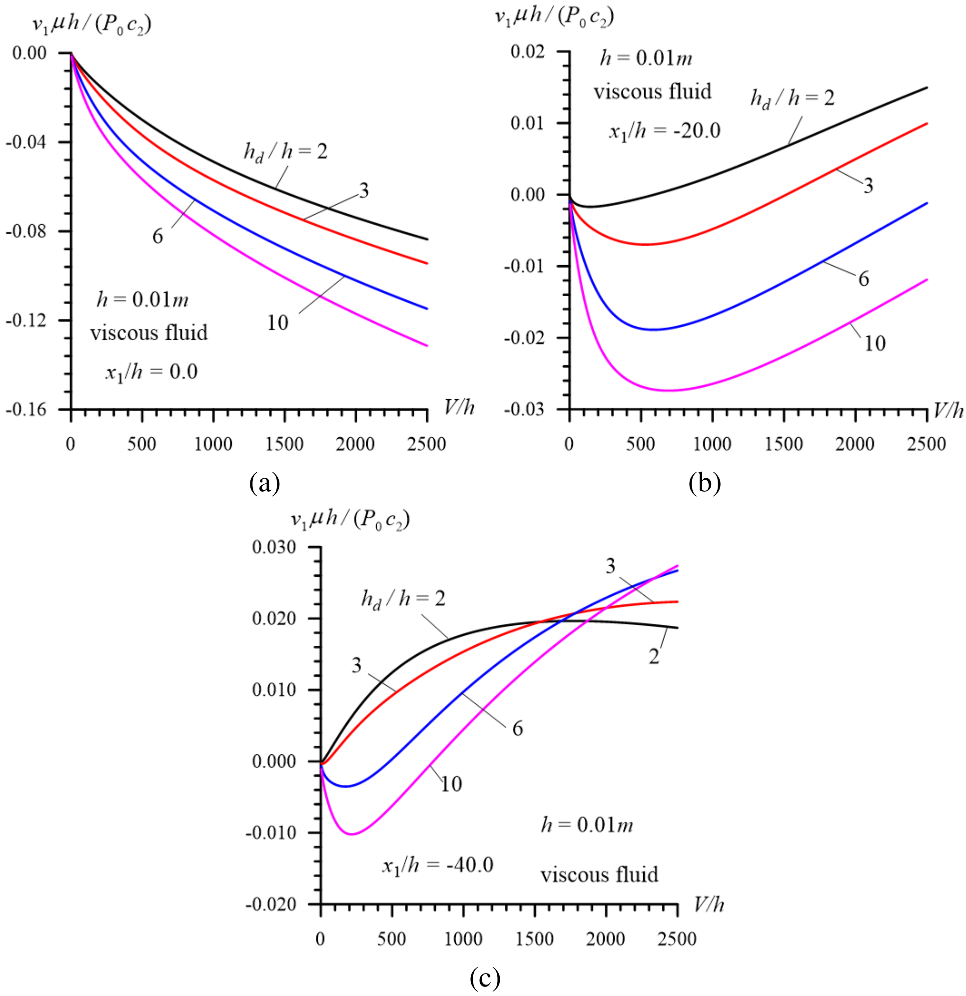

Figure 12: The graphs of the dependence between the velocity $v_1\mu h/(P_0c_2)$ and velocity of the moving load V/h calculated at $x_1/h = 0.0$ (a), -20.0 (b) and -40.0 (c) in the case where $h = 0.01\,m$ for various values of h_d/h

These graphs show that the absolute maximal values of the vertical displacement u_2 of the points of the interface plate decrease with the velocity of the moving load. Some other conclusions from these graphs relating to the character of the vibration of the foundation on which the moving vehicles act, can also be made.

Now we consider the graphs of the dependence between the studied quantities and the velocity V/h. These graphs for the stress $T_{22}h/P_0$ and for the velocities $v_2\mu h/(P_0c_2)$ and $v_1\mu h/(P_0c_2)$ are given in Figs. 10, 11 and 12, respectively and are constructed for the case where $h = 0.01m$ under various h_d/h. In these figures the graphs grouped by letters a, b and c relate to the cases where the values of the stress and velocities are calculated at points $x_1/h =$ 0.0, -20.0 and -40.0, respectively. It follows from these graphs that the character of the dependencies under consideration differs at different points. However, at each point the influence of the fluid viscosity on these dependencies decreases with the velocity of the moving load. In other words, at each selected point the dependencies constructed in the viscous fluid case are close to the corresponding ones with the velocity of the moving load.

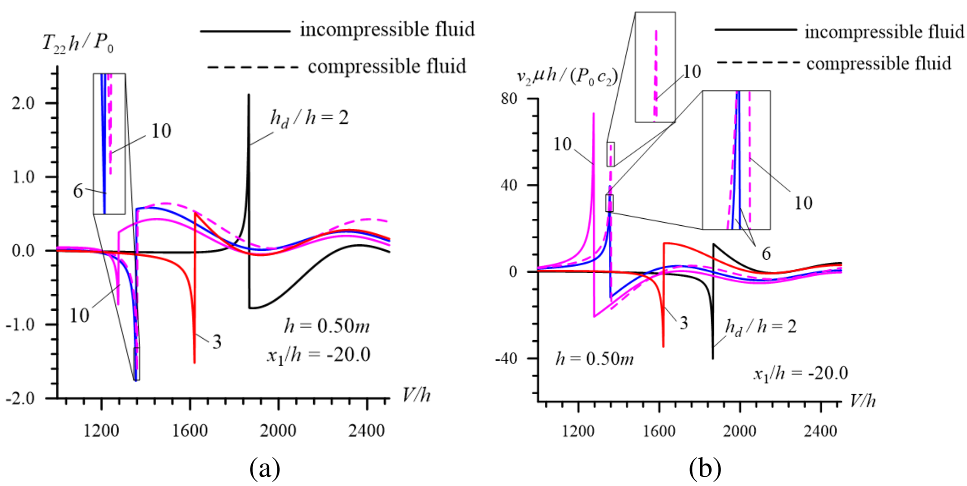

Figure 13: Illustration of the resonance values of the stress $T_{22}h/P_0$(a) and velocity $v_2\mu h/(P_0c_2)$ (b) under the critical velocities of the moving load for various h_d/h arising in the case where $h = 0.50m$ and $x_1/h = -20.0$

All the foregoing results have been obtained within the scope of the compressible viscous and inviscid fluid models. However, results obtained within the scope of the incompressible fluid models for the above-selected values of the problem parameters coincide almost completely with the corresponding ones given above. Now we consider the results which illustrate the influence of the fluid compressibility on the values of the studied quantities.

4.3 The influence of the fluid compressibility on the distribution of the interface stress and velocities

We recall that the influence of the fluid compressibility is characterized through the parameter Ω_1 (20). Numerical results show that the influence of the fluid compressibility on the studied quantities becomes considerable in the cases where $\Omega_1 \geq 0.25$. However, in the cases where $\Omega_1 \geq 0.25$ the influence of the fluid viscosity on the distribution of the stress $T_{22}h/P_0$ and velocity $v_2\mu h/(P_0c_2)$ disappears almost completely. Under obtaining results related to the incompressible fluid model we assume that $\Omega_1 = 0.0$. Based on this reason, we investigate the influence of the fluid compressibility on the values of the studied quantities within the scope of the inviscid fluid case.

Thus, according to the foregoing discussions, an increase in the values of the velocity must increase the difference between the results obtained within the scope of the compressible and incompressible fluid models. However, the investigations show that there exists such a value of the velocity of the moving load under which the absolute values of the studied quantities become infinite and a resonance-type event takes place. As an example of the said event we consider the graphs given in Fig.13 which show the dependence among the stress $T_{22}h/P_0$ (Fig.13a), $v_2\mu h/(P_0c_2)$ (Fig. 13b) and the velocity V/h around the aforementioned critical velocity for various values of h_d/h under $h = 0.5\,m$. Note that under construction of these graphs the values of the stress and velocity are calculated at the point $x_1/h = -20$. Moreover, note that these graphs were constructed for the incompressible fluid case, but as an example, the corresponding graphs for the compressible fluid case which are constructed in the case where $h_d/h = 10$ are also given in Fig. 13.

Note that the existence of the critical velocity is characteristic for dynamics of the moving load acting on the layered medium. A review of the investigations relating to the critical velocity of the moving load acting on bi-material elastic systems was made in a paper by Akbarov and Ilhan (2008). However, up to now, we have not found any investigation on the critical velocity of the moving load action on hydro-elastic systems. Consequently, the results related to the critical velocity, which are discussed here, are the first attempts on the investigations of the critical velocity of the moving load acting on hydro-elastic systems.

We introduce the notation V_{cr}/a_0 for illustration of the values of the dimensionless critical velocity. Numerical investigations show that the values of V_{cr}/a_0 are the same for each studied quantity and for each point, i.e. for each value of x_1/h, where the values of these quantities are calculated. Numerical investigations also show that the values of V_{cr}/a_0 do not depend on the plate thickness h, but depend on the values of the ratio h_d/h and on the compressibility or incompressibility of

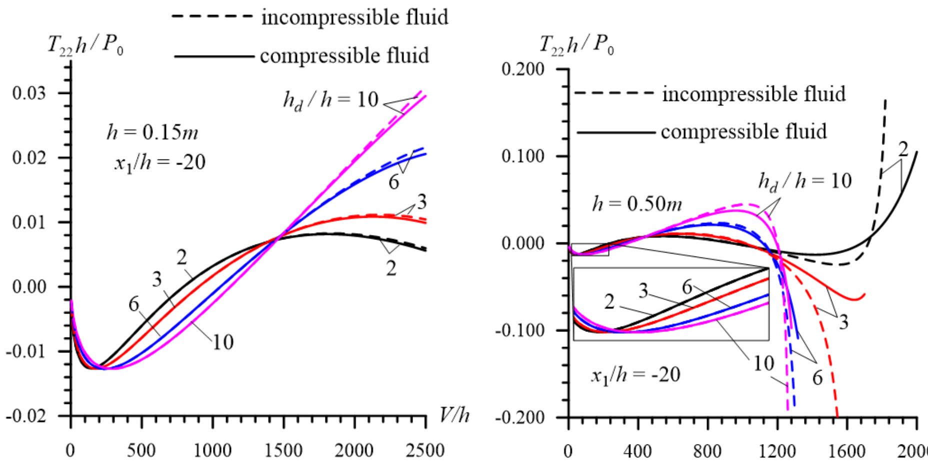

(a) (b)

Figure 14: The influence of the fluid compressibility on the dependence between stress $T_{22}h/P_0$and the velocity of the moving load V/h with various values of h_d/h in the cases where $h = 0.15\,m$ (a) and 0.50 m (b)

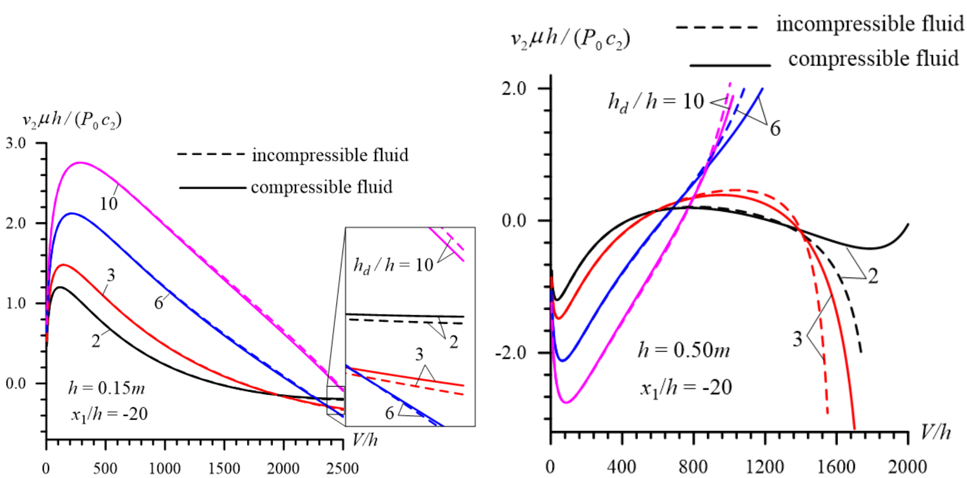

(a) (b)

Figure 15: The influence of the fluid compressibility on the dependence between the velocity $v_2\mu h/(P_0c_2)$ and the velocity of the moving load V/h with various values of h_d/h in the cases where $h = 0.15\,m$(a) and 0.50 m (b)

Table 1: The values of the critical velocity of the moving load. Upper (lower) numbers relate to the case where the fluid is modeled as incompressible (compressible).

Fluids	h_d/h			
	2	3	6	10
Glycerin V_{cr}/a_{0Gl}	$\frac{0.4839}{0.5889}$	$\frac{0.4203}{0.4748}$	$\frac{0.3515}{0.3788}$	$\frac{0.3308}{0.3528}$
Water V_{cr}/a_{0W}	$\frac{0.5606}{1.0011}$	$\frac{0.4809}{0.5912}$	$\frac{0.3891}{0.4304}$	$\frac{0.3550}{0.3842}$

the fluid. Moreover, it is established that the values of V_{cr}/a_0 depend also on the mechanical properties of the fluid and of the plate. Table 1 shows the values of V_{cr}/a_0 calculated for various values of h_d/h. Note that these calculations were made not only for the case where the fluid which filled the strip-space between the plate and rigid wall is Glycerin, but also for the case where this fluid is water for which $\rho_0 = 1000\,kg/m^3$ and $a_0 = 1459.5\,m/s$. Note that in Table 1 through a_{0Gl} and a_{0W} the sound speed in the Glycerin and in the Water, respectively, is denoted. Moreover, in Table 1 the upper (lower) numbers show the values of V_{cr}/a_0 obtained in the case where the corresponding fluid is modeled as incompressible (compressible). Thus, according to the data given in Table 1, we can conclude that the fluid compressibility causes an increase in the values of the critical velocity. However, as a result of the increase in the ratio h_d/h the values of the critical velocity decrease.

Now we consider the graphs of the dependence among $T_{22}h/P_0$, $v_2\mu h/(P_0c_2)$ and the velocity V/h constructed for the compressible and incompressible fluid models in the case where $V/h < V_{cr}/h$. These graphs are given in Figs. 14 (for $T_{22}h/P_0$) and 15 (for $v_2\mu h/(P_0c_2)$) and those grouped by letters a and b indicate the cases where $h = 0.15\,m$ and $0.5m$, respectively. It follows from these graphs that the character of the influence of the fluid compressibility on the values of the studied quantities depends on V/h not only in the quantitative sense but also in the qualitative sense.

5 Conclusions

Thus, in the present paper the dynamics of the moving load acting on the hydro-elastic system consisting of the elastic plate, compressible viscous fluid and rigid wall is investigated. The motion of the plate is described within the scope of the so-called three-dimensional linearized theory of elastic waves in pre-stressed bodies, however, the motion of the fluid is described within the scope of the linearized Navier-Stokes equations. The formulated hydro-elastic problem is solved by employing the moving coordinate system and Fourier transformation with respect to the moving coordinate. Analytical expressions for the Fourier transformation of the sought values are obtained and their originals are determined numerically. Numerical results related to the interface normal stress and velocities are presented and discussed. According to these discussions, the following concrete conclusions related to the mechanics of the studied problem are established:

- the influence of the fluid viscosity on the distribution of the studied quantities increases with decreasing fluid depth, plate thickness and velocity of the moving load;

- as a result of the fluid viscosity the distribution of the studied quantities with respect to the moving coordinate along the moving direction becomes non-symmetric with respect to the point at which the moving load acts;

- according to the determination of the moving coordinates, the aforementioned distributions with respect to the moving coordinate are also taken as the change of the studied quantities with respect to time at some fixed interface point;

- in the cases where the influence of the fluid viscosity on the studied quantities is considerable, the influence of the fluid compressibility on these quantities is negligible;

- the influence of the fluid compressibility on the studied quantities appears under high velocities of the moving load, and this influence increases with plate thickness and with fluid depth;

- according to the foregoing conclusions, under high velocities of the moving load the influence of the fluid compressibility on the studied normal stress and on the velocity of the interface point in the direction of the normal to the interface plane, can be studied within the scope of the inviscid fluid model;

- it is established that for the selected pair of plate and fluid materials there exists the critical velocity of the moving load under which the resonance-type event takes place and the absolute values of the studied quantities become infinite;

- it is also established that the values of the critical velocity decrease with the fluid depth. At the same time, the compressibility of the fluid causes the values of the critical velocity to increase.

References

Akbarov, S. D. (2013a): On the axisymmetric time-harmonic Lamb's problem for a system comprising a half-space and a covering layer with finite initial strains. *CMES: Computer Modeling in Engineering & Science*, vol. 70, pp. 93 – 121.

Akbarov, S. D. (2013b): Frequency response of a pre-stressed elastic metal plate under compressible viscous fluid loading. Non-Newtonian System in the Oil and Gas Industry, Proceedings of the International Scientific Conference devoted to the 85^{th} Anniversary of Academician Azad Khalil oglu Mirzajanzadeh, Baku, pp. 21-22.

Akbarov, S. D. (2015): *Dynamics of pre-strained bi-material systems: linearized three-dimensional approach*. Springer.

Akbarov, S. D.; Ilhan, N. (2008): Dynamics of a system comprising a pre-stressed orthotropic layer and pre-stressed orthotropic half-plane under action of a moving load. *International Journal of Solids and Structures,* vol. 45, no. 14, pp. 4222 – 4235.

Akbarov, S. D.; Ilhan, N. (2013): Time harmonic Lamb's problem for a system comprising piezoelectric layer and piezoelectric half-plane. *Journal Sound and Vibration*, vol. 332, pp. 5375-5392.

Akbarov, S. D.; Hazar, E.; Eroz, M. (2013): Forced vibration of the plate strip resting on a rigid foundation. *CMC: Computers, Materials & Continua*, vol. 36, no. 1, pp. 23 – 48.

Akbarov, S. D.; Ismailov, M. I. (2014a): Forced vibration of a system consisting of a pre- strained highly elastic plate under compressible viscous fluid loading. *CMES: Computer Modeling in Engineering & Science* , vol. 97, no. 4, pp. 359 – 390.

Akbarov, S. D.; Ismailov, M. I. (2014b): Frequency response of a viscoelastic plate under compressible viscous fluid loading. *International Journal of Mechanics*, vol. 8, pp. 332 – 344.

Bagno, A. M.; Guz, A. N.; Shchuruk, G. L. (1994); Influence of fluid viscosity on waves in an initially deformed compressible elastic layer interacting with a fluid medium. *International Applied Mechanics*, vol. 30, no. 9, pp. 643-649.

Bagno, A. M.; Guz, A. N. (1997): Elastic waves in prestressed bodies interacting with fluid (Survey). *International Applied Mechanics,* vol. 33, no. 6, pp. 435-465.

Charman, C. J.; Sorokin, S. V. (2005): The forced vibration of an elastic plate under significant fluid loading. *Journal Sound and Vibration*, vol. 281, pp. 719-741

Fu, Y.; Price, W. (1987): Interactions between a partially or totally immersed vibrating cantilever plate and surrounding fluid. *Journal Sound and Vibration*, vol. 118, no. 3, pp. 495- 513.

Fu, S.; Cui, W.; Chen, X.; Wang, C. (2005): Hydroelastic analysis of a nonlinearity connected floating bridge subjected to moving loads. *Marine Structures,* vol. 18, pp. 85 – 107.

Guz, A. N. (2009): *Dynamics of compressible viscous fluid.* Cambridge Scientific

Publishers.

Guz, A. N.; Makhort, F. G. (2000): The physical fundamentals of the ultrasonic nondestructive stress analysis of solids. *International Applied Mechanics*, vol. 36, pp. 1119 – 1148.

Guz, A. N. (2004): *Elastic waves in bodies with initial (residual) stresses.* Kiev; A.C.K. (in Russian).

Kwak, H.; Kim, K. (1991): Axisymmetric vibration of circular plates in contact with water. *Journal Sound and Vibration*, vol. 146, pp. 381-216.

Lamb, H. (1921): Axisymmetric vibration of circular plates in contact with water. *Proc. R Soc. (London)* A, vol. 98, pp. 205-216.

Sorokin, S. V.; Chubinskij, A. V. (2008): On the role of fluid viscosity in wave propagation in elastic plates under heavy fluid loading. *Journal Sound and Vibration*, vol. 311, pp. 1020-1038.

Tubaldi, E.; Armabili, M. (2013): Vibrations and stability of a periodically supported rectangular plate immersed in axial flow. *Journal Fluids and Structures*, vol. 39, pp. 391- 407.

Wang, C.; Fu, S.; Cui, W. (2009): Hydroelasticity based fatigue assessment of the connector for a ribbon bridge subjected to a moving load. *Marine Structures,* vol. 22, pp. 246 – 260.

Wu, J. S.; Shih, P. Y. (1998): Moving-load-induced vibrations of a moored floating bridge. *Computer & Structures,* vol. 66, no. 4, pp. 435 – 461.

Zhao, J.; Yu, S. (2012) Effect of residual stress on the hydro-elastic vibration on circular diaphragm. *World Journal of Mechanics,* vol. 2, pp. 361-368.